







Proceedings of ICACTCE'21

High School of Technology, Moulay Ismail University Meknes, Morocco, and
Faculty of Sciences and Techniques Mohammeda, Hassan II University, Morocco
March 24 – 26, 2021, Morocco

Editors: Mariyam Ouaisa, Mariyam Ouaisa, Sarah El Himer, and Zakaria Boulouard

Research Article

Far Field Prediction From Near Field Using the Plane Wave Spectrum Method

Mohamed Amine Benchana¹ , Abderrezak Khalfallaoui¹ , Abdelhalim Chaabane¹ ,
Abdesselam Babouri*² , Abdelaziz Ladjimi²  and Zouheir Riah³

¹Department of Electronics and Telecommunications, Université 8 Mai 1945 Guelma, Guelma, Algeria

²Department of Electrical and Automatic Engineering, Université 8 Mai 1945 Guelma, Guelma, Algeria

³IRSEEM, Ecole supérieure d'ingénieurs ESIGELEC, Rouen, France

Abstract. Over the past decade, the evolution of embedded system has taken place drastically as it has been for their integration in various industries. This increases *Electro-Magnetic Interferences* (EMI) problems and generates new design constraints on *Electro-Magnetic Compatibility* (EMC). Thus, the nature of the electromagnetic environment and the prospective for undesired coupling must be taken into consideration by embedded systems engineers to avoid the equipment failure or malfunction. Accordingly, the radiated emission models are of great interest to designers of electronic equipment. This paper exploits the *Plane Wave Spectrum* (PWS) technique to predict and compute the magnetic field at various distances till 100 mm above a *Device Under Test* (DUT). Good similarities are obtained between the magnetic field components calculated by PWS and the simulated ones by HFSS at different elevation from the electric dipole.

Keywords. Electromagnetic Compatibility (EMC); Near-field; Far-field; Plane Wave Spectrum (PWS)

PACS. 41.20.-q; 25.30.Mr; 13.40.-f

Copyright © 2020 Mohamed Amine Benchana, Abderrezak Khalfallaoui, Abdelhalim Chaabane, Abdesselam Babouri, Abdelaziz Ladjimi and Zouheir Riah. *This is an open access article distributed under the Creative Commons Attribution License, which permits unrestricted use, distribution, and reproduction in any medium, provided the original work is properly cited.*

1. Introduction

Nowadays, the EMI problems have increased in a dramatic way. This resulted mainly from the high level of integration of embedded electronic systems in a confined space together with

*Corresponding author: abdesselam.babouri@gmail.com

the increasing of operating frequencies and the switching speeds in high performance modern equipment such as: mobile phone, electric engine and automotive vehicle, etc. [7,8]. Hence, all of these factors tend to increase EMI and generate undesired currents peaks or voltages in certain parts of the integrated system which could cause equipment to malfunction or failure. Thus, the knowledge of the electromagnetic behavior and the environment of components becomes indispensable to overcome these technical issues and guarantee the quality of the systems. For this purpose, several methods [2–6, 9, 10] have been proposed in the literature to model, predict and characterize the radiated emissions of the electronic component that may affect other components near it.

In [3,9], two different models were developed and tested to model the radiated emission: the model based on electric dipoles and the model based on magnetic dipoles. Furthermore, in [10] the equivalent radiating model was improved by using an optimization algorithm and image processing. Subsequently, a simple electromagnetic modeling procedure to integrate the model into a commercial electromagnetic simulator was reported in [5]. Authors in [4] used a single model to predict the electromagnetic conducted emission of a microcontroller. Other approaches were proposed in the literature to model the radiated emission, and to predict the EM field emitted by the DUT from the near field measurement, by applying either the neural network method [2], or the PWS technique as authors reported in [6, 11].

In this paper, we choose to employ the near-field/far-field transformation using the plane wave spectrum method [1, 12] for the modeling process. This technique which allows us to calculate the magnetic field at several heights above the DUT is applied and used to predict the radiated magnetic field at the best possible height above an elementary electric dipole placed in XY plane with radiation frequency of 2 GHz. Section 2 presents the theory of the PWS. Whereas section 3 discusses the obtained results. Finally, this paper concludes with the presentation of the achieved results and the future works.

2. Plane Wave Spectrum Theory

In a source-free free-space region, the time-harmonic Maxwell equations can be transformed into the following vector wave equations [12]:

$$\begin{cases} \nabla^2 \mathbf{E} + k^2 \mathbf{E} = 0, \\ \nabla^2 \mathbf{H} + k^2 \mathbf{H} = 0, \end{cases} \quad (2.1)$$

$$\nabla \cdot \mathbf{E} = \nabla \cdot \mathbf{H} = 0. \quad (2.2)$$

The general solution of the above equation for $z \geq 0$ can be represented as a superposition of plane waves with the same frequency propagating in different directions.

$$\vec{H}(x, y, z) = \frac{1}{4\pi^2} \int_{-\infty}^{\infty} \int_{-\infty}^{\infty} \vec{F}(k_x, k_y) \exp(-j\vec{k} \cdot \vec{r}) dk_x dk_y, \quad (2.3)$$

$$\vec{H}(x, y, z) = \frac{1}{4\pi^2} \int_{-\infty}^{\infty} \int_{-\infty}^{\infty} [\vec{F}(k_x, k_y) e^{-jk_z z}] \exp(-j(k_x x + k_y y)) dk_x dk_y. \quad (2.4)$$

From (2.4) the following inverse Fourier transform can be derived:

$$\vec{F}(k_x, k_y) = \frac{1}{4\pi^2} \int_{-\infty}^{\infty} \int_{-\infty}^{\infty} \vec{H}(x, y, z) \cdot \exp(j(k_x x + k_y y)) dx dy, \tag{2.5}$$

where k_x and k_y are real variables.

With $\vec{k} = k_x \vec{u}_x + k_y \vec{u}_y + k_z \vec{u}_z$ and $\vec{r} = x\vec{u}_x + y\vec{u}_y + z\vec{u}_z$.

\vec{k} is the wave vector and \vec{r} is the position vector.

In equations (2.3) and (2.4), F represents a uniform *Plane Wave Spectrum* (PWS) of the magnetic field that propagate in the direction k .

$$\vec{H}(x, y, z) = \vec{F}(\vec{k}) \exp(-j\vec{k} \cdot \vec{r}). \tag{2.6}$$

Inserting equation (2.6) in (2.2) leads to equation (2.7).

$$F_z(k) = \frac{-(F_x(k)k_x + F_y(k)k_y)}{k_z}. \tag{2.7}$$

Equation (2.4) shows that to calculate the magnetic field at any height along z , the spectrum at the same height must be known. Moreover, the spectrum at any distance along z can be found from the spectrum at $z = z_1$ by using (2.8).

From (2.5) we note that the PWS calculation from the field corresponds to two-dimensional inverse Fourier transform and (2.4) shows that the field calculation from the PWS corresponds to a two-dimensional direct Fourier transform [12].

$$\vec{F}(\vec{k})|_{z=z_2} = \vec{F}(\vec{k})|_{z=z_1} \exp(-jk_z(z_2 - z_1)). \tag{2.8}$$

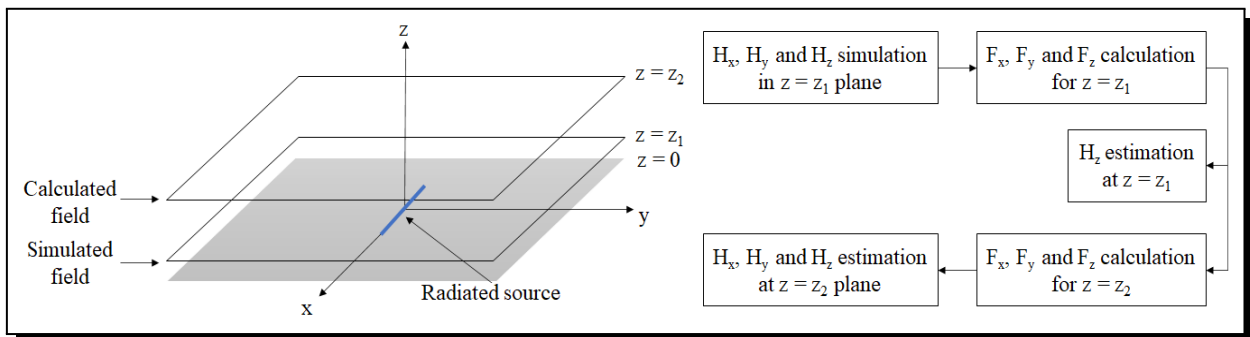


Figure 1. PWS modeling approach

The modeling process is presented in Figure 1, where the radiated source is placed in $z = 0$ and the planar scanning used for H_x , H_y and H_z simulation is conducted to a plane defined at $z = z_1$ near the source. Then the calculation process will be implemented in MATLAB to obtain the field at any height $z > z_1$.

For $z > 0$, the radiation condition requires

$$k_z = \begin{cases} \sqrt{k^2 - k_x^2 - k_y^2}, & \text{if } k_x^2 + k_y^2 \leq k^2, \\ -j\sqrt{k_x^2 + k_y^2 - k^2}, & \text{otherwise.} \end{cases} \tag{2.9}$$

Imaginary k_z correspond to an evanescent PWS which is rapidly attenuated away from the $z = 0$ plane.

3. Results and Discussion

The DUT is represented by an electric dipole placed in the XY-plane and characterized by a current of 100 mA. Its dimensions are very negligible compared to the wavelength. In order to obtain the magnetic near-field, we insert the dipole in a 3D electromagnetic radiation tool that applies a numerical calculation method to resolve Maxwell equations and therefore calculate the radiated field by the dipole. In this work, HFSS (High Frequency Structure Simulator) of Ansoft is the software used to extract the magnetic near field cartographies at a frequency of 2 GHz and at 1 mm (initial height z_1) above the electric dipole. After obtaining all the magnetic field components (H_x , H_y and H_z) at $z = 1$ mm, we can now apply the PWS technique by following the modeling technique presented in Figure 1 to calculate the magnetic field at several distances. However, first an estimation of H_z component at 1 mm is carried out in Figure 2 by using equation (2.7). The cartographies have an area of 100×100 mm with 121×121 simulation points.

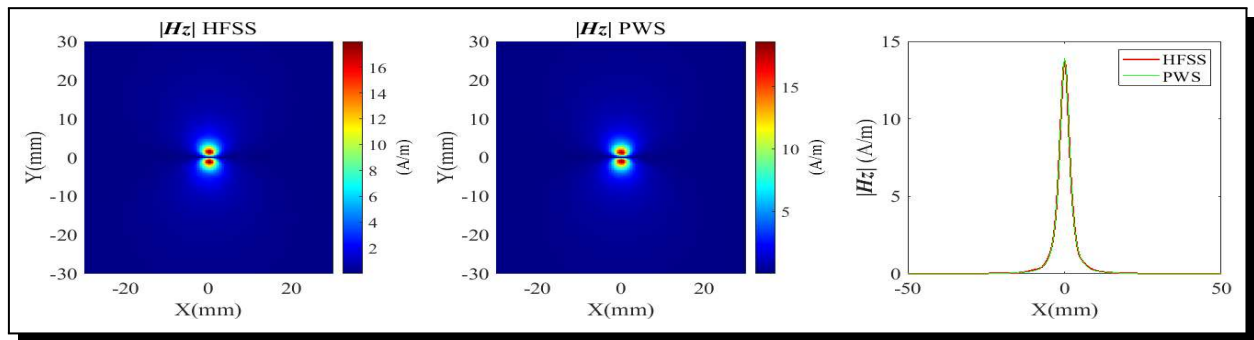


Figure 2. H_z components obtained in simulation and with PWS at 1 mm

According to Figure 2 that indicates a comparison between the H_z component of the magnetic field obtained from HFSS, and the one calculated with the PWS approach, it is clear that they are identical in profile and amplitude with a negligible difference estimated by 0.0013.

From the near field cartography and by applying the PWS theory, the magnetic field can be calculated at several heights $z > 1$ mm above the electric dipole. The results are presented in Figure 3, Figure 4 and Figure 5 for $z = 10$ mm, 50 mm and 100 mm, respectively. Furthermore, an error criterion between the cartographies of the simulated field obtained from HFSS and those obtained from PWS approach is presented in Table 1.

The relative error is calculated using the following expression:

$$\text{error} = \sum_{i=1}^n \frac{1}{|H_{\text{simulated}}(M_i)|^2} |H_{\text{simulated}}(M_i) - H_{\text{PWS}}(M_i)|^2. \quad (3.1)$$

Figure 3 shows that the magnetic field components calculated by the PWS at 10 mm are coherent in profile and amplitude with the ones simulated by HFSS at the same height, with acceptable differences as reported in Table 1.

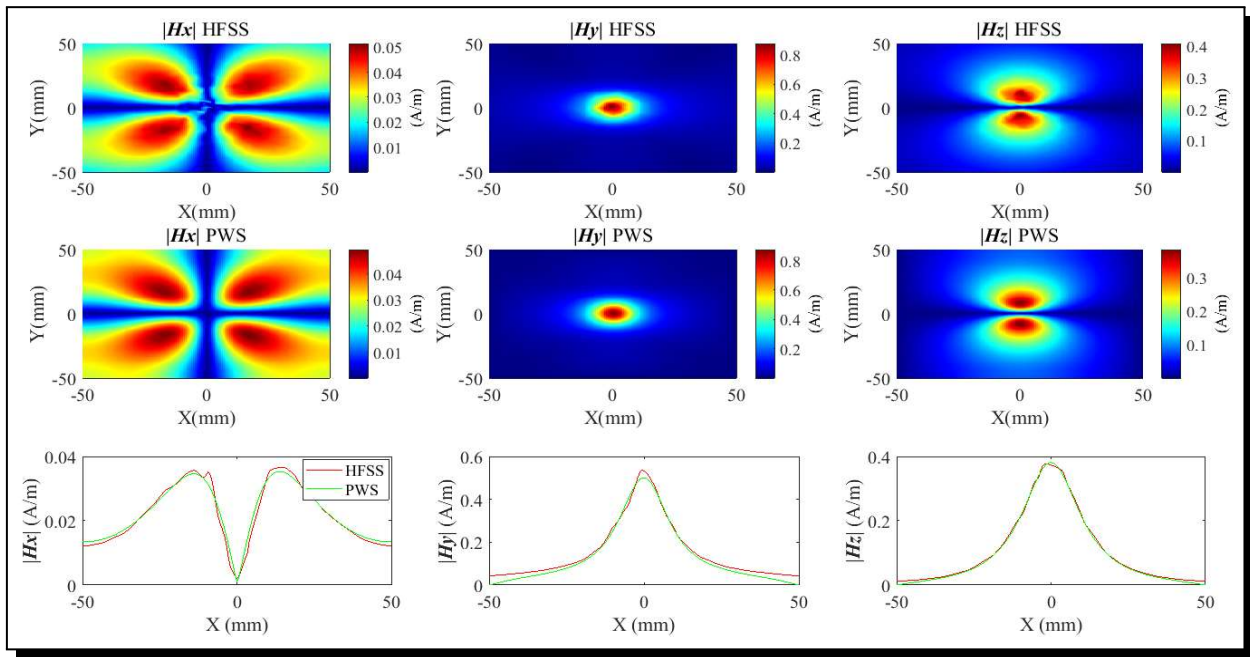


Figure 3. Magnetic field of the three components at 10 mm

Table 1. Errors on the three components of the field calculated by PWS at different heights

Distances	H_x	H_y	H_z
$z = 10 \text{ mm}$	8.7427×10^{-5}	0.0014	6.921×10^{-4}
$z = 50 \text{ mm}$	2.4865×10^{-4}	0.0031	5.1868×10^{-4}
$z = 100 \text{ mm}$	0.001	0.0057	0.0026

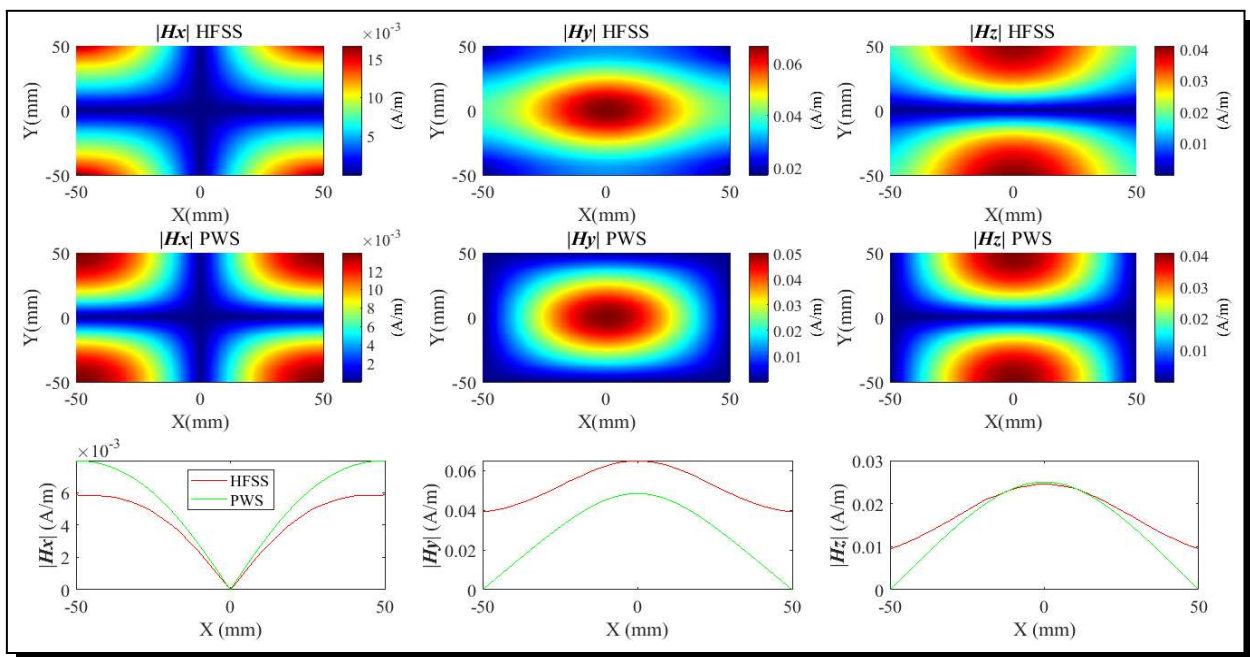


Figure 4. Magnetic field of the three components at 50 mm

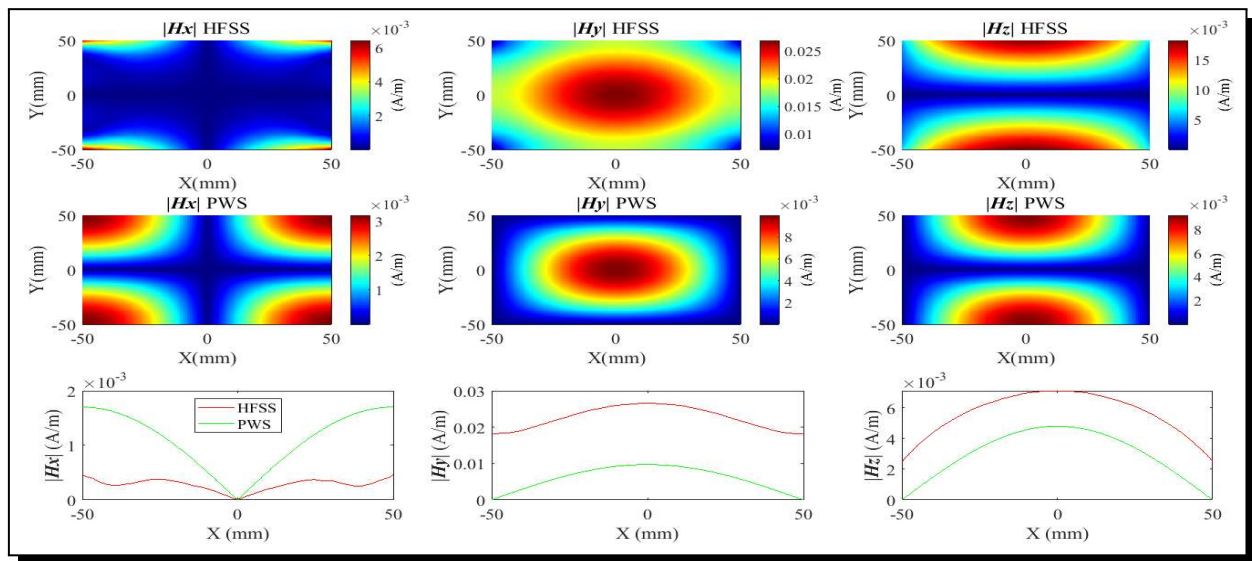


Figure 5. Magnetic field of the three components at 100 mm

For $z = 50$ mm, the field cartographies calculated by the PWS still show a good agreement with the simulated ones with some differences occurring especially in the extremities for lower-field values (see Figure 4). These differences are amplified when the magnetic field is characterized at a higher elevation above the electric dipole, (see Figure 5 for $z = 100$ mm). These differences are significantly rise e.g., ten times higher in the error value of the H_x component at 100 mm compared to its value at 10 mm (see Table 1). Although, they are still reasonable and we can state that the model gives good results.

4. Conclusion

The PWS method that enables near-field/far-field transformation is presented and reported in this paper. The pre-described technique is applied to predict the radiated emission of an electric dipole at various distances. A good agreement is achieved between the calculated results by the PWS method and the simulated ones with negligible differences. Compared to the simulation results obtained from HFSS, a dispersion was observed in the results calculated by the PWS method at planes far from the dipole under test. The approach we have proposed is very effective for studying electromagnetic interference and field prediction. Finally, we suggest to extend this study for many dipoles and to expand the examined zone in the future works.

Acknowledgment

This work is supported by the Directorate General for Scientific Research and Technological Development (DG-RSDT) of Algeria, as part of research project (PRFU No. A01L07UN2401201 90001). A sincere thank you to Mrs. Benchana Samiha for her diligent proofreading of this paper.

Competing Interests

The authors declare that they have no competing interests.

Authors' Contributions

All the authors contributed significantly in writing this article. The authors read and approved the final manuscript.

References

- [1] C.A. Balanis, *Antennas Theory Analysis and Design*, 4th edition, John Wiley & Sons, Inc. (2015), URL: <https://www.wiley.com/enus/Antenna+Theory%3A+Analysis+and+Design%2C+4th+Edition-p-9781119178996>.
- [2] R. Brahimi, A. Kornaga, M. Bensetti, D. Baudry, Z. Riah, A. Louis and B. Mazari, Postprocessing of near-field measurement based on neural networks, *IEEE Transactions on Instrumentation and Measurement* **60** (2011), 539 – 546, DOI: 10.1109/TIM.2010.2050373.
- [3] Y.V. Gilabert, Modélisation des émissions rayonnées de composants électroniques, Mémoire de thèse, Université de Rouen (2007), URL: <http://www.theses.fr/2007ROUES025>.
- [4] C. Labussiere-Dorgan, S. Bendhia, E. Sicard, J. Tao, H.J. Quaresma, C. Lochot and B. Virgnon, Modeling the electromagnetic emission of a microcontroller using a single model, *IEEE Transactions on Electromagnetic Compatibility* **50** (2008), 22 – 34, DOI: 10.1109/TEMC.2007.911918.
- [5] P.F. Lopez, C. Arcambal, D. Baudry and S. Verdeyme, Simple electromagnetic modeling procedure: from near-field measurements to commercial electromagnetic simulation Tool, *IEEE Transactions on Instrumentation and Measurement* **59** (2010), 3111 – 3121, DOI: 10.1109/TIM.2010.2063070.
- [6] Z. Riah, *Caractérisation et Modélisation des Phénomènes Radiatifs en Champ Proche des Composants et des Dispositifs Electroniques*, Rapport HDR, Université de Rouen (2015), URL: <https://hal.archives-ouvertes.fr/tel-02435179/>.
- [7] T. Sandu, O.T. Nedelcu and M. Gologanu, Electromagnetic Interference Shielding Assessment from Mixing Formulae, 2020 *International semiconductor Conference (CAS)* (2020), 221 – 224, Sinaia, Romania, DOI: 10.1109/CAS50358.2020.9267992.
- [8] H.H. Slim, S. Braun, E. Gulten, A. Frech and P. Russer, Automated measurement of intermittent signals using a time domain EMI measurement system, 2009 *IEEE International Symposium on Electromagnetic Compatibility* (2009), 232 – 235, Austin, TX, DOI: 10.1109/ISEMC.2009.5284582.
- [9] Y. Vives, C. Arcambal, A. Louis, F. de Daran, P. Eudeline and B. Mazari, Modeling magnetic radiations of electronic circuits using near-field scanning method, *IEEE Transactions on Electromagnetic Compatibility* **49** (2007), 391 – 400, DOI: 10.1109/TEMC.2006.890168.
- [10] Y. Vives, C. Arcambal, A. Louis, P. Eudeline and B. Mazari, Modeling magnetic emissions combining image processing and optimization algorithm, *IEEE Transactions on Electromagnetic Compatibility* **51** (2009), 909 – 918, DOI: 10.1109/TEMC.2009.2032171.
- [11] V. Volski, B. Ravelo, V. A. E. Vandenbosch and D. Pissort, Investigation on planar near-to-far-field transformations for EMC applications, 9th *European Conference on Antennas and Propagation (EuCAP)* (2015), 1 – 5, Lisbon, URL: <https://ieeexplore.ieee.org/document/7228733>.
- [12] J.J.H. Wang, An Examination of the theory and practices of planar near-field measurement, *IEEE Transactions on Antennas and Propagation* **36** (1988), 746 – 753, DOI: 10.1109/8.1176.

